Journal of Arrhythmia 30 (2014) 433–438

Contents lists available at ScienceDirect

Journal of Arrhythmia

journal homepage: www.elsevier.com/locate/joa

Original Article

Spatial and transmural repolarization, and dispersion of repolarization and late potentials evaluated using signal-averaged vector-projected 187-channel high-resolution electrocardiogram in Brugada syndrome

Kimie Ohkubo, MD[a], Ichiro Watanabe, MD[a,*], Yasuo Okumura, MD[a], Masayoshi Kofune, MD[a], Koichi Nagashima, MD[a], Hiroaki Mano, MD[a], Kazumasa Sonoda, MD[a], Toshiko Nakai, MD[a], Yuji Kasamaki, MD[a], Atsushi Hirayama, MD[a], Naokata Sumitomo, MD[b], Tomohiro Nakayama, MD[c]

[a] Division of Cardiology, Department of Medicine, Nihon University School of Medicine, Tokyo, Japan
[b] Department of Pediatrics, Nihon University School of Medicine, Tokyo, Japan
[c] Department of Laboratory Medicine, Nihon University School of Medicine, Tokyo, Japan

ARTICLE INFO

Article history:
Received 23 July 2013
Received in revised form
18 October 2013
Accepted 25 October 2013
Available online 22 December 2013

Keywords:
Brugada syndrome
Recovery time
Late potential
Spatial dispersion

ABSTRACT

Background: Vector-projected 187-channel electrocardiograms (ECGs) were recorded in 45 patients with a Brugada-type ECG to evaluate spatial and transmural repolarization and dispersion of action potential duration in Brugada syndrome (BS).
Methods: Corrected recovery time (RT-c, R wave peak to the first positive maximum derivative of the T wave with Bazett correction) and RT-c dispersion were calculated. The corrected T peak-end interval (T(p-e)-c, T wave peak to the end of the T wave with Bazett correction) and T(p-e)-c dispersion were calculated.
Results: RT-c dispersion and T(p-e)-c interval were longer in patients with a type 1 ECG, but there was no significant difference in Tp-e dispersion between patients with a type 1 and those with a type 2/3 ECG. No significant correlation was noted between RT-c dispersion, T(p-e)-c dispersion, and symptoms. Late potentials ($P=0.023$) and a family history of sudden cardiac death ($P=0.0017$) were correlated with symptoms.
Conclusions: Spatial dispersion of repolarization may constitute the electrocardiographic pattern of the Brugada type ECG and conduction disturbance in addition to repolarization abnormality may contribute to the development of malignant ventricular tachyarrhythmias.

1. Introduction

Brugada syndrome (BS) is an arrhythmogenic entity characterized by the presence of ST-segment elevation in leads V1–V3 on surface electrocardiogram (ECG), the absence of structural heart disease, and a high risk of ventricular tachycardia/ventricular fibrillation (VT/VF) and sudden cardiac death (SCD) [1–3]. Risk stratification is controversial, especially in asymptomatic individuals [4–6]. Transmural dispersion of repolarization within the ventricular myocardium has been suggested to underlie arrhythmogenesis in BS [7], and ECG markers of ventricular repolarization have been reported for the identification of high-risk patients with BS [8]. We investigated whether ECG-based spatial and transmural ventricular depolarization and repolarization values are potential risk factors for arrhythmic events in BS patients. In the present study, we used the recently developed signal-averaged vector-projected 187-channel high-resolution ECG (187-channel SAVP-ECG).

2. Methods

2.1. Study patients

The study group comprised 45 consecutive patients (male/female ratio: 43/2; mean age, 51.5 ± 14.4 years) with spontaneous ($n=26$) or drug-induced (pilsicainide 1 mg/kg) ($n=19$) type 1 BS ECG phenotype. The ECG diagnosis of BS was based strictly on the recommendations of the Second Consensus Conference [3]. Structural heart disease was ruled out in all study patients by performing transthoracic echocardiography. Those with a history of syncope, documented sustained ventricular arrhythmia,

* Correspondence to: Division of Cardiology, Department of Medicine, Nihon University School of Medicine, 30-1 Oyaguchi-kamimachi, Itabashi-ku, Tokyo 173-8610, Japan. Tel.: +81 3 3972 8111; fax: +81 3 3972 1098.
E-mail address: watanabe.ichirou@nihon-u.ac.jp (I. Watanabe).

1880-4276/$ - see front matter © 2013 Japanese Heart Rhythm Society. Published by Elsevier B.V. All rights reserved.
http://dx.doi.org/10.1016/j.joa.2013.10.004

or aborted SCD were considered symptomatic. The study was approved by the Institutional Review Committee of Nihon University Hospital, and the patients signed informed consent for 187-channel SAVP-ECG recording, mutation screening for the SCN5A gene, and invasive electrophysiological study.

2.2. 187-channel SAVP ECG

187-channel SAVP-ECGs were obtained with an electrode lead system, an input box, a high-precision amplifier (HRES-1000, Fukuda Denshi Co. Ltd., Tokyo, Japan), and a personal computer. The input box generated a modified *X*–*Y*–*Z*-lead ECG, and the vector-projected 187-channel synthesized ECGs via a Mason–Likar lead system. The input signal ($\pm$550 mV) was digitized at 2 kHz by an analog-to-digital (A/D) converter with a resolution of 0.076 μV. Ten electrodes were attached to the right shoulder, left shoulder, left lower abdomen, right lower abdomen, and the usual V1–V6 recording sites. The 187-channel SAVP-ECG recording was performed with patients in a resting position. Details of the187-channel SAVP-ECG have been reported previously [9–11]. The 187-channel SAVP-ECG variables measured in the current study are described below.

2.3. Repolarization

The RT interval was defined as the time between the peak of the R wave and the maximum positive peak of the first derivative of the T wave, which was defined as the peak of the T wave. The RT end interval (RTend) was defined as the time between the peak of the R wave and the maximum negative derivative of the T wave. T peak-end (T(p-e)) was defined as the time between the T peak and the maximum negative derivative of the T wave (Fig. 1). RT dispersion was automatically calculated as the difference between the longest RT interval (RTmax) and the shortest RT interval (RTmin). RTend dispersion was automatically calculated as the difference between the longest RTend interval (RTend max) and the shortest RTend interval (RTend min). T peak-end dispersion was also automatically calculated as the difference between the longest T peak-end interval (Tp-e max) and the shortest T peak-end interval (Tp-e min). The corrected RT interval (RT-c), corrected RTend interval (RTend-c), and corrected T peak-end interval (T(p-e)-c) were calculated according to the Bazett formula. Average RT-c, average RTend-c, and average T(p-e)-c were calculated as the average value of each of these variables as detected on the 187-channel SAVP-ECG. Formulas for the variables are as follows:

Average RT-c = average of each RT-c
RT-c dispersion = RT-c max − RT-c min
Average RTend-c = average of each RTend-c
RTend-c dispersion = RTend-c max − RTend-c min
Average T(p-e)-c = average of each T(p-e)-c
T(p-e)-c dispersion = T(p-e)-c max − T(p-e)-c min
Average RT-c dispersion = average of (each RT-c − RT min-c)
Average RTend-c dispersion = average of (each RTend-c − RTend min-c)
Average T(p-e)-c dispersion = average of [each T(p-e)-c − T(p-e)-c min]

The RTc, RTe-c, and T(p-e)-c maps were displayed as 256-color coordinated maps according to the time difference. In brief, blue represents $<$ 40 ms; green-yellow, 40 − 79 ms; orange, 80 − 99 ms; and red $\geq$ 100 ms.

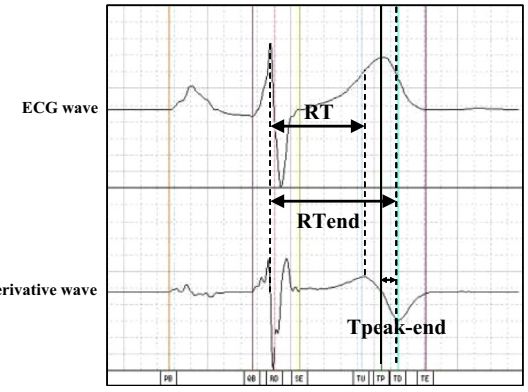

Fig. 1. Reference point for RT interval, T peak-end interval, and RTend interval. The RT interval was defined as the time between the peak point of the R wave and the positive maximum peak of the first derivative of the T wave. The T peak-end was defined as the time between the peak point of the T wave and the negative maximum peak of the first derivative of the T wave. RTend was defined as the time between the peak point of the R wave and the negative maximum peak of the first derivative of the T wave (modified from Nakai et al. [9]).

2.4. Depolarization

The modified *X*–*Y*–*Z*-lead ECG and the synthesized signals from the 187-channel SAVP-ECGs were amplified and passed through a finite impulse response (FIR) digital filter (frequency characterization: 27th order) with a low frequency of 45 Hz and a high frequency of 280 Hz, and then A/D converted with 12-bit accuracy at 2000 samples/s. After rejection of ectopic beats, ECG signals over 10 min were averaged by means of the signal-processing system. The non-filtered *X*–*Y*–*Z*-lead ECG, filtered *X*–*Y*–*Z*-lead ECG, and vector magnitude ECG were displayed on the same time scale (Fig. 1). The filtered QRS (fQRS) duration was determined automatically according to the beginning and end of the vector magnitude ECG by the points exceeding 5 times the noise levels. The root mean square of the last 40 ms (RMS_{40}) was measured by the integrated magnitude at 40 ms before the QRSend of the vector magnitude ECG. In addition, we measured the duration of low-amplitude signals $<$ 40 μV (LAS_{40}) on the vector magnitude ECG. Spatial distribution of integrated high-frequency late potentials (HFLPs), as shown by 187-channel SAVP-ECG mapping, was calculated as the integration of the electrical potentials of fQRS measured between 30 ms (initial offset) before the QRSend (QRSend-30) and the QRSend. The endpoint in each channel was defined as the endpoint of the QRS, where the average exceeded the mean plus 5 standard deviations of the noise sample. The integrated HFLP map based on the 187-channel SAVP-ECGs was defined graphically by the gray scale that exceeded 5 times the mean noise level. The spatial distribution of integrated HFLPs based on the 187-channel SAVP-ECGs was superimposed on the RTc and T(p-e)-c dispersion map (Fig. 2).

2.5. Electrophysiological study

A comprehensive electrophysiological study was performed in 27 patients in a fasting, drug-free, non-sedated state. For patients who underwent coronary artery stent implantation, programmed ventricular stimulation was performed at 1 month after stent implantation. After obtaining access to the right femoral vein at 4 sites, 1 quadripolar catheter (Biosense-Webster, Diamond Bar, CA, USA) was positioned at the right atrial appendage, 1 octapolar catheter (Biosense-Webster) was positioned at the his bundle electrogram recording site, and 2 steerable quadripolar catheters (6 F) with an interelectrode distance of 2–5–2 mm (Biosense-Webster) were positioned in the right ventricular apex and outflow tract. Endocardial potentials were filtered to recording frequencies of 30 − 500 Hz and recorded on a BARD computer system (BARD Lab Pro, BARD Electrophysiology, Lowell, MA, USA). Programmed electrical stimulation

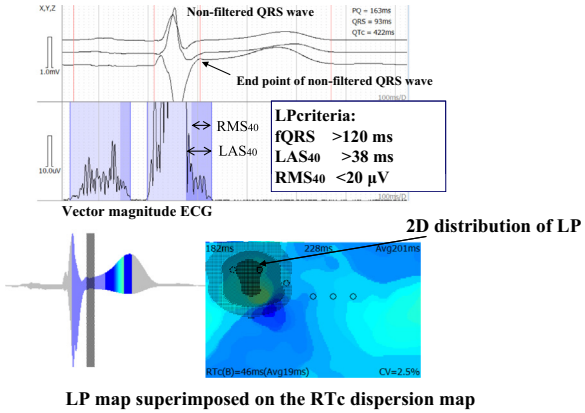

Fig. 2. Spatial distribution of high frequency ventricular late potentials (HFLPs) as defined by the gray scale on the RT dispersion map based on a 187-channel signal-averaged vector-projected high-resolution electrocardiogram. HFLPs were generated graphically by dividing voltages that exceeded 5 times the mean noise level, and represented by an increasing gray scale. The HFLP area is variable depending on the threshold voltage, which can be changed in 0.5 μV steps. Note the high frequency late potentials located at the right anterior lesion. The RTc dispersion map was displayed as a 256-color coordinated map according to the time differences. In brief, the blue represents < 40 ms; green-yellow, 40 – 79 ms; orange, 80 – 99 ms; and red, ≥ 100 ms. LP, ventricular late potential; fQRS, filtered QRS duration; RMS_{40}, root mean square of the last 40 ms; LAS_{40}, duration of low amplitude signals < 40 μV; RTc, time between the peak point of the R wave and the positive maximum peak of the first derivative of the T wave corrected using the Bazett formula.

from the right ventricular apex and right ventricular outflow tract was performed at twice the diastolic threshold strength and a pulse of 2-ms duration with a pulse generator (BD-02, Fukuda Denshi Co.). An S_1–S_2 interval was applied after 8 beats of drive pacing (S_1) at basic cycle lengths of 600 ms and 400 ms. The S_1–S_2 interval was decreased in 10-ms steps until the effective refractory period of the right ventricle was reached. When ventricular fibrillation (VF) lasting > 5 s and requiring DC shock was not induced with a single premature beat, 3 extra stimuli (S_2 until the effective refractory period was reached, S_3 and S_4 to 180 ms) were delivered.

2.6. Follow-up

In general, patients were followed up at 4- to 5-month intervals in our outpatient clinic. Examinations included assessment of subjective symptoms and 12-lead ECG and device interrogation if necessary in the event of onset of symptoms or device discharges. Follow-up ranged from 36 to 214 months (mean, 80.8 ± 52.3 months; median, 91 months).

2.7. Statistical analysis

Continuous clinical and electrophysiological values are shown as mean ± SD. Between-group differences in these values were analyzed using the Mann–Whitney *U* test. Categorical data were analyzed by Fisher's exact probability test. A *P* value of < 0.05 was considered statistically significant. StatView 5.0 software (SAS Institute Inc., Cary, NC, USA) was used for analysis.

3. Results

The clinical, genetic, electrocardiographic, and electrophysiological characteristics of the study patients are shown in Table 1. Eight of the 45 patients were symptomatic, having a history of syncope (n=3) or aborted SCD (n=5). The remaining 37 patients were asymptomatic, although 4 had a family history of SCD. The ECGs of 26 patients showed a type 1 basal ECG pattern, and 19 showed a type 1 ECG pattern after a challenge test. An SCN 5 A mutation was found in 1 patient. Positive ventricular late potentials were detected in 26 of 44 (59.1%) patients. Among the 28 patients in whom an electrophysiological study was performed, VF was induced in 25 (89.3%). The clinical, genetic, electrocardiographic, and electrophysiological characteristics of the patients in each group (symptomatic and asymptomatic patients) are shown in Table 2. A family history of sudden cardiac death (SCD) at age < 45 years, spontaneous type 1 ECG, and positive ventricular late potentials were significantly more prevalent in the group of symptomatic patients. However, the AH interval, HV interval, and inducibility of VF/polymorphic VT did not differ between the 2 groups of patients.

Table 1
Clinical, genetic, electrocardiographic, and electrophysiological characteristics of the study patients (n=45).

Age (y); mean ± SD	51.5 ± 14.3
Sex ratio (M/F)	43/2
Symptomatic	8
Cardiopulmonary arrest	5
Syncope	3
Family history of SCD	4
Spontaneous Brugada type 1 ECG pattern	26
SCN5A gene mutation	1
Late potential; mean ± SD	26/44 (59.1%)
EPS	28
AH interval (ms); mean ± SD	101.5 ± 22.7
HV interval (ms); mean ± SD	47.4 ± 9.2
Inducible VF/PVT at EPS	25
ICD implantation	10
Follow-up (mo); mean ± SD	80.8 ± 52.3
Arrhythmic event during follow-up	1

Number of patients is shown unless otherwise indicated.
SCD, sudden cardiac death; EPS, electrophysiological study; VF, ventricular fibrillation; PVT, polymorphic ventricular tachycardia; ICD, implantable cardioverter defibrillator.

3.1. Spatial and transmural repolarization obtained from 187-channel SAVP-ECG

The average RT-c, RTend-c, and T(p-e)-c intervals calculated from the 187-channel SAVP-ECG are shown in Table 3. The average T(p-e)-c was marginally increased in patients with a type 1 ECG compared to that in patients with a type 2/3 ECG (49.0 ± 14.1 ms vs. 41.0 ± 8.1 ms, P=0.062). However, no significant difference between average RTend-c and average T(p-e)-c intervals was observed.

3.2. Spatial and transmural dispersion of repolarization obtained from 187-channel SAVP-ECG

RT-c dispersion was significantly greater in patients with a type 1 ECG compared to that in patients with a type 2/3 ECG (86.3 ± 20.8 ms vs. 73.3 ± 19.7 ms, P=0.041). Additionally, average RT-c dispersion was greater in patients with a type 1 ECG compared to that in patients with a type 2/3 ECG (41.8 ± 15.8 ms vs. 32.4 ± 16.8 ms, P=0.064) (Table 4, Figs. 3 and 4). However, no significant difference in RTe-c dispersion, average RTe-c dispersion, T(p-e)-c dispersion, or average T(p-e) dispersion was observed between the type 1 and type 2/3 ECG patterns. No significant difference in RT-c dispersion, average RT-c dispersion, RTe-c dispersion, average RTe-c dispersion, T(p-e) dispersion, or average T(p-e) dispersion was observed between symptomatic and asymptomatic patients (Table 4).

An arrhythmic event occurred in 1 symptomatic patient during the follow-up period.

4. Discussion

In the present study, we showed that average T(p-e)-c interval, RT-c dispersion, and corrected average repolarization dispersion were greater in patients with a type 1 ECG than in patients with a type 2/3 ECG. However, no differences were noted in other variables representing other parameters of repolarization interval and spatial and transmural dispersion of repolarization between patients with a type 1 and those with a type 2/3 ECG. Furthermore, no differences in spatial and transmural dispersion variables were observed between symptomatic and asymptomatic patients, although the prevalence of positive late ventricular potentials was significantly higher in symptomatic patients. The prevalence of positive ventricular late potential in type 1 ECG was marginally higher compared to that in type 2/3 ECG (16/26 vs. 6/18, $P=0.062$), and both repolarization and depolarization abnormalities may constitute a type 1 ECG. Qualitative analysis showed that late potentials were located adjacent to the V_2–V_3 ECG position, whereas the distribution of the RT-c, RTe-c, and T(p-e)-c

Table 2
Clinical, genetic, electrocardiographic, and electrophysiological characteristics of symptomatic and asymptomatic patients.

	Symptomatic ($n=8$)	Asymptomatic ($n=37$)	*P* value
Age (y); mean ± SD	56.0 ± 16.0	49.2 ± 13.1	0.18
Sex ratio (M/F)	8/0	35/2	0.50
Family history of SCD	3	1	0.014
Spontaneous Brugada type 1 ECG pattern	8	18	0.0072
Late potential	7/8	16/36	0.023
SCN5A gene mutation	1	0	0.178
EPS	8	19	0.014
AH interval (ms); mean ± SD	92.9 ± 9.2	105.1 ± 25.8	0.36
HV interval (ms); mean ± SD	48.5 ± 3.8	47.7 ± 11.1	0.66
Inducible VF/PVT at EPS	8/8	17/19	0.34
ICD implantation	5	5	0.0025
Follow-up (mo); mean ± SD	124 ± 65	71.5 ± 45.0	0.0005
Arrhythmic event during follow-up	1	0	Not applicable

Number of patients is shown unless otherwise indicated.
SCD, sudden cardiac death; EPS, electrophysiological study; VF, ventricular fibrillation; PVT, polymorphic ventricular tachycardia; ICD, implantable cardioverter defibrillator.

Table 3
Comparison of spatial and transmural repolarization time and Brugada ECG type and symptoms.

	Avg. RT-c	Avg. RTe-c	Avg. T(p-e)-c
BS Type 1 ECG	215.7 ± 24.5	312.9 ± 24.0	49.0 ± 14.1
BS Type 2/3 ECG	215.1 ± 27.9	301.4 ± 33.2	41.0 ± 8.1
***P* value**	0.93	0.11	0.062
Symptomatic	213.9 ± 40.3	310.4 ± 35.3	48.5 ± 11.1
Asymptomatic	215.8 ± 21.0	307.5 ± 52.8	45.2 ± 12.9
***P* value**	0.47	0.73	0.41

RT-c, corrected recovery time interval; Avg., average; RTe-c, corrected recovery time end interval; T(p-e), T peak-end interval.
See the text for the definition of these parameters.

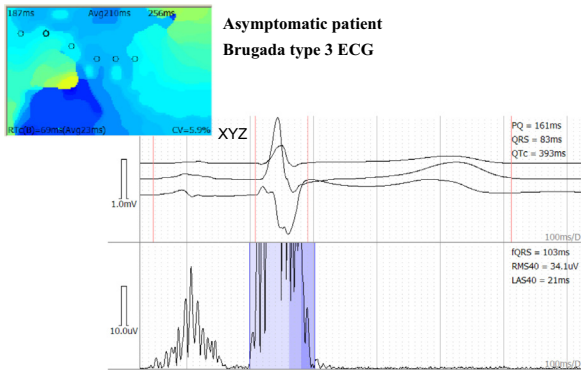

Fig. 3. RTc dispersion map in an asymptomatic patient with a Brugada type 3 ECG. Color scale is as described in Fig. 2. RTc dispersion is 69 ms, and average RTc dispersion is 23 ms. The ventricular late potential is negative. Abbreviations are as in Fig. 2.

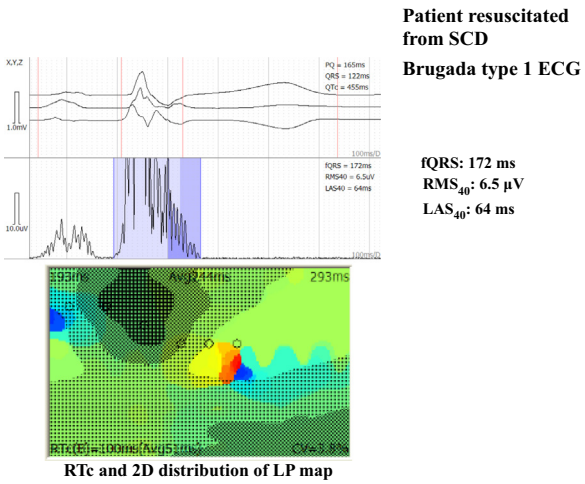

Fig. 4. RTc dispersion map in a symptomatic case with a Brugada type 1 ECG. Color scale is as in Fig. 2. RTc dispersion is 100 ms and average RTc dispersion is 51 ms. The ventricular late potential is positive. Abbreviations are as in Fig. 2.

Table 4
Comparison of spatial and transmural dispersion of repolarization and Brugada ECG type and symptoms.

	RT-c dispersion	Avg. RT-c dispersion	RTe-c dispersion	Avg. RTe-c dispersion	T(p-e)-c dispersion	Avg. T(p-e)-c dispersion
BS Type 1 ECG	86.3 ± 20.8	41.8 ± 15.8	64.2 ± 18.0	37.6 ± 17.8	62.4 ± 19.3	37.6 ± 18.7
BS Type 2/3 ECG	73.3 ± 19.7	32.4 ± 16.8	73.3 ± 19.7	33.8 ± 10.9	58.8 ± 13.3	35.8 ± 11.8
***P* value**	0.041	0.064	0.17	0.42	0.49	0.72
Symptomatic	77.6 ± 28.4	41.3 ± 17.4	67.8 ± 13.1	30.9 ± 12.7	59.6 ± 19.7	27.6 ± 13.7
Asymptomatic	81.9 ± 19.6	37.4 ± 16.7	60.1 ± 16.9	37.2 ± 15.8	61.3 ± 16.7	38.8 ± 16.1
***P* value**	0.61	0.56	0.24	0.30	0.80	0.74

RT-c, corrected recovery time interval; Avg., average; RTe-c, corrected recovery time end interval; T(p-e), T peak-end interval.
See the text for the definition of these parameters.

dispersion was more widespread, and usually located left inferior to the late potential location. The dispersion of the depolarization and repolarization indices suggests a different pathogenesis of these abnormalities.

Transmural dispersion of repolarization within the ventricular myocardium has been suggested to underlie arrhythmogenesis in Brugada, short QT, or long QT syndrome, and in SCD [12,13]. Three electrophysiologically distinct cell types have been identified in the ventricular myocardium: endocardial, epicardial, and M cells. Differences in the time course of repolarization of these 3 ventricular myocardial cell types contribute prominently to inscription of the electrocardiographic T-wave [14]. In isolated ventricular wedge preparations, the peak of the T-wave was shown to coincide with epicardial repolarization and the end of the T-wave with repolarization of the M cells; thus, Tp-e provides a measure of transmural dispersion of repolarization [15]. These and other studies have suggested that although Tp-e on the surface ECG may not be equivalent to transmural dispersion of repolarization, this interval may serve as an index of transmural dispersion of repolarization and thus be helpful in forecasting risk for the development of life-threatening arrhythmias [13,15]. Evidence in support of this hypothesis has been provided in hypertrophic cardiomyopathy, congenital, and acquired long QT syndrome, and other pathologic conditions [7]. The reported cellular basis of BS is marked dispersion of repolarization in the right ventricular epicardium and transmurally [16–18]. Previous studies showed that the T peak-end interval and T peak-end dispersion on the 12-lead ECG are potential risk factors for VT/VF and VT/VF inducibility in patients with the Brugada ECG phenotype [8,19]. Studies have reported that QT/RR and T peak-end/RR slopes show loss of rate-dependency in VF(+) BS patients than in VF(−) BS patients and control patients, and the T peak-end interval correlated negatively with the RR interval in the VF(+) Brugada group and positively with the RR interval in the VF(−) Brugada and control groups [20]. However, an experimental study comparing epicardial electrograms and surface electrograms showed that T peak-end does not correlate with transmural dispersion of repolarization but rather is an index of total dispersion of repolarization [21]. In the present study, average T(p-e)-c interval, corrected maximum T peak-end dispersion, and corrected average T peak-end dispersion from the 187-channel SAVP-ECG did not differ between symptomatic and asymptomatic BS patients. However, average T(p-e)-c interval was marginally increased in patients with type 1 ECG compared to that in patients with type 2/3 Brugada type ECG. Additionally, corrected maximum RT interval dispersion and corrected average RT interval dispersion were greater in patients with a type 1 ECG compared to those in patients with a type 2/3 Brugada type ECG. However, the parameters on the absolute value and dispersion of repolarization did not differ between symptomatic and asymptomatic BS patients. Therefore, the ECG manifestation of type 1 Brugada ECG may be related to the longer transmural repolarization interval and greater spatial dispersion of refractoriness. Recent studies have shown that right ventricular fibrosis and conduction delay without a transmural repolarization gradient are the dominant pathophysiologic mechanisms for type 1 ECG and the origin of VF in BS [22–25]. We previously reported the presence of right ventricular outflow tract endocardial conduction delay and right ventricular septal histopathological abnormalities in patients with BS [26,27]. Furthermore, Nademanee et al. reported that the electrophysiological mechanism in patients with BS is delayed depolarization over the anterior aspect of the right ventricular outflow tract, and catheter ablation of this area of abnormal depolarization results in normalization of the Brugada ECG pattern and prevents VT/VF [28]. In our patient series, the prevalence of ventricular late potentials was significantly higher in symptomatic patients than in asymptomatic patients.

4.1. Study limitations

Our study was limited first by the fact that the 187-channel SAVP-ECG is not yet widely accepted for assessment of spatial and transmural dispersion of repolarization; therefore, further studies may be needed to validate this novel ECG algorithm. Second, the study group was small. A subsequent study involving a large study group is needed to verify the clinical usefulness of the 187-channel SAVP-ECG.

5. Conclusion

Spatial dispersion of repolarization may constitute the electrocardiographic pattern of the Brugada type ECG, and this conduction disturbance in addition to repolarization abnormality may contribute to the development of malignant ventricular tachyarrhythmias.

Conflict of interest

None.

References

[1] Brugada P, Brugada J. Right bundle branch block, persistent ST segment elevation and sudden cardiac death: a distinct clinical and electrocardiographic syndrome. A multicenter report. J Am Coll Cardiol 1992;20:1391–6.
[2] Benito B, Brugada R, Brugada J, et al. Brugada syndrome. Prog Cardiovasc Dis 2008;51:1–22.
[3] Antzelevitch C, Brugada P, Borggrefe M, et al. Brugada syndrome: report of the second consensus conference: endorsed by the Heart Rhythm Society and the European Heart Rhythm Association. Circulation 2005;111:659–70.
[4] Priori SG, Napolitano C, Gasparini M, et al. Clinical and genetic heterogeneity of right bundle branch block and ST-segment elevation syndrome: a prospective evaluation of 52 families. Circulation 2000;102:2509–15.
[5] Eckardt L, Probst V, Smits JP, et al. Long-term prognosis of individuals with right precordial ST-segment-elevation Brugada syndrome. Circulation 2005;111:257–63.
[6] Brugada J, Brugada R, Brugada P. Determinants of sudden cardiac death in individuals with the electrocardiographic pattern of Brugada syndrome and no previous cardiac arrest. Circulation 2003;108:3092–6.
[7] Antzelevitch C. Role of spatial dispersion of repolarization in inherited and acquired sudden cardiac death syndrome. Am J Physiol Heart Circ Physiol 2007;293:H2024–38.
[8] Castro Hevia J, Antzelevitch C, Tornés Barzaga F, et al. Tpeak-Tend and Tpeak-Tend dispersion as risk factors for ventricular tachycardia/ventricular fibrillation in patients with the Brugada syndrome. J Am Coll Cardiol 2006;47:1828–34.
[9] Nakai K, Tsuboi J, Okabayashi H, et al. Development of a signal-averaged vector-projected 187-channel high-resolution electrocardiogram for the evaluation of the spatial location of high-frequency potentials and abnormal ventricular repolarization. Int Heart J 2007;48:701–13.
[10] Nakai K, Miyake F, Kasanuki H, et al. Newly developed signal-averaged vector-projected 187-channel electrocardiogram can evaluate the spatial distribution of repolarization heterogeneity. Int Heart J 2008;49:153–64.
[11] Suzuki A, Shiga T, Nakai K, et al. Interlead difference between T-peak to T-end intervals in resynchronization patients with an implantable cardioverter–defibrillator. J Electrocardiol 2010;43:706–12.
[12] Antzelevitch C. Tpeak-Tend interval as an index of transmural dispersion of repolarization. Eur J Clin Invest 2001;31:555–7.
[13] Panikkath R, Reinier K, Uy-Evanado A, et al. Prolonged Tpeak-to-Tend interval on the resting ECG is associated with increased risk of sudden cardiac death. Circ Arrhythm Electrophysiol 2011;4:441–7.
[14] Yan GX, Antzelevitch C. Cellular basis for the normal T wave and the electrocardiographic manifestation of the long QT syndrome. Circulation 1998;98:1928–36.
[15] Fish JM, Di Diego JM, Nesterenko V, et al. Epicardial activation of left ventricular wall prolongs QT interval and transmural dispersion of repolarization: implications for biventricular pacing. Circulation 2004;109:2136–42.
[16] Yan GX, Antzelevitch C. Cellular basis for the Brugada syndrome and other mechanisms of arrhythmogenesis associated with ST-segment elevation. Circulation 1999;100:1660–6.
[17] Aiba T, Shimizu W, Hidaka I, et al. Cellular basis for trigger and maintenance of ventricular fibrillation in the Brugada syndrome model. J Am Coll Cardiol 2006;47:2074–85.
[18] Morita H, Zipes DP, Fukushima-Kusamo K, et al. Repolarization heterogeneity in the right ventricular outflow tract: correlation with ventricular arrhythmias in Brugada patients and in an in vitro Brugada model. Heart Rhythm 2008;5:725–33.

[19] Letsas KP, Weber R, Asthemer K, et al. Tpeak-Tend interval and Tpeak-Tend/QT ratio as markers of ventricular tachycardia inducibility in subjects with Brugada ECG phenotype. Europace 2010;12:271–4.
[20] Sangawa M, Morita H, Nakatsu T, et al. Abnormal transmural repolarization process in patients with Brugada syndrome. Heart Rhythm 2009;6:1163–9.
[21] Opthof T, Coronel R, Wilms-Schopman FJ, et al. Dispersion of repolarization in canine ventricle and the electrocardiographic T wave: Tp-e interval does not reflect transmural dispersion. Heart Rhythm 2007;4:341–8.
[22] Coronel R, Casini S, Koopmann TT, et al. Right ventricular fibrosis and conduction delay in a patient with clinical signs of Brugada syndrome. A combined electrophysiological, genetic, histopathologic, and computational study. Circulation 2005;112:2769–77.
[23] Postema PG, van Dessel PF, de Bakker JM, et al. Slow and discontinuous conduction conspire in Brugada syndrome: a right ventricular mapping and simulation study. Circ Arrhythm. Electrophysiol 2008;1:379–86.
[24] Postema PG, van Dessel PF, Kors JA, et al. Local depolarization abnormalities are the dominant pathophysiologic mechanism for type 1 electrocardiogram in Brugada syndrome: a study of electrocardiograms, vectorcardiograms, and body surface potential maps during ajmaline provocation. J Am Coll Cardiol 2010;55:789–97.
[25] Hoogendijk MG, Potse M, Linnenbank AC, et al. Mechanism of right precordial ST-segment elevation in structural heart disease: excitation failure by current-to-load mismatch. Heart Rhythm 2010;7:238–48.
[26] Ohkubo K, Watanabe I, Takagi Y, et al. Endocardial electrograms from the right ventricular outflow tract after induced ventricular fibrillation in patients with Brugada syndrome. Circ J 2007;71:1258–62.
[27] Ohkubo K, Watanabe I, Okumura Y, et al. Right ventricular histological substrate and conduction delay in patients with Brugada syndrome. Int Heart J 2010;51:17–23.
[28] Nademanee K, Veerakul G, Chadanamattha P, et al. Prevention of ventricular fibrillation episodes in Brugada syndrome by catheter ablation over the anterior right ventricular outflow tract epicardium. Circulation 2011;123:1270–9.